

See discussions, stats, and author profiles for this publication at: <https://www.researchgate.net/publication/221735268>

Ablation of ceramide synthase 2 strongly affects biophysical properties of membranes

Article in *Journal of Lipid Research* · March 2012

DOI: 10.1194/jlr.M022715 · Source: PubMed

CITATIONS

64

READS

111

9 authors, including:



Liana C Silva

University of Lisbon

82 PUBLICATIONS 2,852 CITATIONS

SEE PROFILE



Oshrit Ben-David

Ben-Gurion University of the Negev

9 PUBLICATIONS 568 CITATIONS

SEE PROFILE



Elad Lavee

BioLineRx

18 PUBLICATIONS 1,477 CITATIONS

SEE PROFILE



Johnny Stiban

Birzeit University

30 PUBLICATIONS 1,115 CITATIONS

SEE PROFILE

Some of the authors of this publication are also working on these related projects:



1) Co-evolution of pentameric ligand-gated ion channels and sterols 2) Nanoscopy of neurotransmitter receptors in synapses. [View project](#)



Fluorescence studies of acetylcholine receptor [View project](#)

Ablation of ceramide synthase 2 strongly affects biophysical properties of membranes^S

Liana C. Silva,^{1,*†,§} Oshrit Ben David,[†] Yael Pewzner-Jung,[†] Elad L. Laviad,[†] Johnny Stiban,^{2,†} Sibali Bandyopadhyay,^{**} Alfred H. Merrill, Jr.,^{**} Manuel Prieto,[§] and Anthony H. Futerman[†]

iMed.UL,* Research Institute for Medicines and Pharmaceutical Sciences, Faculdade de Farmácia, Universidade de Lisboa, 1649-003 Lisboa, Portugal; Department of Biological Chemistry,[†] Weizmann Institute of Science, Rehovot 76100, Israel; CQFM & IN,[§] Instituto Superior Técnico, 1049-001 Lisboa, Portugal; and School of Biology and Petit Institute for Bioengineering and Bioscience,^{**} Georgia Institute of Technology, Atlanta, GA 30332-0230

Abstract Little is known about the effects of altering sphingolipid (SL) acyl chain structure and composition on the biophysical properties of biological membranes. We explored the biophysical consequences of depleting very long acyl chain (VLC) SLs in membranes prepared from lipid fractions isolated from a ceramide synthase 2 (CerS2)-null mouse, which is unable to synthesize C22–C24 ceramides. We demonstrate that ablation of CerS2 has different effects on liver and brain, causing a significant alteration in the fluidity of the membrane and affecting the type and/or extent of the phases present in the membrane. These changes are a consequence of the depletion of VLC and unsaturated SLs, which occurs to a different extent in liver and brain. In addition, ablation of CerS2 causes changes in intrinsic membrane curvature, leading to strong morphological alterations that promote vesicle adhesion, membrane fusion, and tubule formation. Together, these results show that depletion of VLC-SLs strongly affects membrane biophysical properties, which may compromise cellular processes that critically depend on membrane structure, such as trafficking and sorting.—Silva, L. C., O. Ben David, Y. Pewzner-Jung, E. L. Laviad, J. Stiban, S. Bandyopadhyay, A. H. Merrill, Jr., M. Prieto, and A. H. Futerman. **Ablation of ceramide synthase 2 strongly affects biophysical properties of membranes.** *J. Lipid Res.* 2012. 53: 430–436.

Supplementary key words ceramide • sphingolipids • acyl chain • lipid domains • tubules • membrane order

Sphingolipids (SLs) are important components of biological membranes and are involved in a variety of biological functions. SL synthesis starts at the endoplasmic reticulum

This work was supported by Compromisso para a Ciência 2008, by Grant PTDC/QUI-BIQ/I11411/2009 from Fundação para a Ciência e Tecnologia (FCT, Portugal), by Israel Science Foundation Grant 1735/07, and by National Institutes of Health Grant GM076217. L.C.S. was supported by Compromisso para a Ciência 2008. A.H.F. is the Joseph Meyerhoff Professor of Biochemistry at the Weizmann Institute of Science.

Manuscript received 17 November 2011 and in revised form 5 January 2012.

Published, JLR Papers in Press, January 9, 2012
DOI 10.1194/jlr.M022715

(1) with the formation of ceramide (Cer), the backbone of all complex SLs (2). In mammals, Cer consists of a fatty acid of variable chain length linked by an amide bond to C-2 of the long-chain base, sphinganine, or sphingosine. *N*-acylation of the long-chain base is catalyzed by a family of six ceramide synthases (CerS), each of which uses a relatively restricted subset of acyl CoAs for *N*-acylation (3). For instance, CerS1 and CerS5 use long acyl chain CoAs (C18- and C16-, respectively), whereas CerS2 and CerS3 are involved in the synthesis of very long acyl chain SLs (>C22) (4). Additionally, the expression pattern of CerS is cell specific, which is reflected in the different SL acyl chain composition in a given tissue (5).

We recently generated a CerS2 null mouse (6). This mouse that lacks very long acyl chain ceramides and SLs (C22–C24) displays severe pathology, including hepatopathy (7) and encephalopathy (8). The cellular mechanisms that cause these pathologies have not been fully elucidated, but alterations in membrane lipid composition are likely to affect diverse cellular functions, including trafficking, cell-cell communication, signal transduction, and protein function (9, 10), which themselves may depend to a large extent on the biophysical properties of cell membranes. Indeed, activation of several signaling cascades has been ascribed to the presence of different type of membrane domains, including lipid rafts and Cer-platforms (11, 12) and/or structural alterations in membranes (13). Preliminary observations demonstrated changes in the membrane biophysical properties of liver membranes in

Abbreviations: Cer, ceramide; CerS, ceramide synthase; GUV, giant unilamellar vesicle; HexCer, hexosylceramide; LC, long chain; LCB, long-chain base; NBD, 1,2-Dipalmitoyl-sn-glycero-3-phosphoethanolamine-N-(7-nitro-2-1,3-benzoxa-diazol-4-yl); Rho, 1,2-Dioleoyl-sn-Glycero-3-Phosphoethanolamine-N-(Lissamine Rhodamine B Sulfonyl); SL, sphingolipid; t-PnA, trans-parinaric acid; VLC, very long chain.

¹To whom correspondence should be addressed.

e-mail: lianacsilva@ff.ul.pt

²Current address: Department of Biology and Biochemistry, Birzeit University, P.O. Box 14, West Bank, Palestinian Authority.

^SThe online version of this article (available at <http://www.jlr.org>) contains supplementary data in the form of two figures.

the CerS2 null mouse (6), including increased fluidity and strong morphological alterations.

We have performed a systematic analysis of the biophysical properties of membrane lipids isolated from the two main tissue types that show pathology in the CerS2 null mouse, namely brain and liver. Membrane biophysical properties were studied by fluorescence spectroscopy and microscopy. Our results demonstrate that ablation of CerS2 has different effects on different tissues, causing significant alterations in global membrane order through changes in the type and/or extent of the phases present in the membrane and drives changes in membrane morphology, promoting adhesion and fusion of neighboring vesicles. These changes are a consequence of the depletion of very long chain (VLC) and unsaturated SLs, which occurs to a different extent in liver and brain.

MATERIALS AND METHODS

Materials

Rho (1,2-Dioleoyl-*sn*-Glycerol-3-Phosphoethanolamine-*N*-(Lissamine Rhodamine B Sulfonyl)) was obtained from Avanti Polar Lipids (Alabaster, AL). NBD (1,2-Dipalmitoyl-*sn*-glycerol-3-phosphoethanolamine-*N*-(7-nitro-2-*l*,3-benzoxa-diazol-4-yl)) and *trans*-parinaric acid (t-PnA) were from Molecular Probes (Leiden, The Netherlands). All organic solvents were UVASOL grade from Merck.

Preparation of lipid extracts

Tissue was homogenized in 20 mM HEPES (pH 7.4), 0.2 mM EGTA, 420 mM mannitol, and 150 mM sucrose. Homogenates were centrifuged at 400 g_{av} for 10 min, and the supernatant was collected and centrifuged at 8,500 g_{av} for 10 min. The subsequent supernatant was centrifuged at 100,000 g_{av} for 1 h. The pellet was suspended in the same buffer, and lipids were extracted (14).

Lipid analysis

SLs were measured by ESI-MS/MS using a PE-Sciex API 3000 triple quadrupole mass spectrometer and an ABI 4000 quadrupole-linear ion trap mass spectrometer (4, 6, 15). SL levels were normalized to pmol/mg of dry weight, and data were plotted as a molar fraction of total SLs using $X_i = n_i / \sum n_i$, where X_i is the molar fraction of the lipid i , and n is the number of moles of the lipid i .

Confocal fluorescence microscopy

Fluorescence microscopy experiments were performed at room temperature using a Leica TCS SP5 (Leica Microsystems CMS GmbH, Mannheim, Germany) inverted microscope (DMI6000) with a 63 \times water (1.2 numerical aperture) apochromatic objective. Giant unilamellar vesicles were prepared by electroformation (16) using microsomal lipid extracts from liver or brain. Rho and NBD were used to label the vesicles at a final concentration of 1 μ M and 5 μ M, respectively.

Fluorescence measurements

Multilamellar lipid vesicles (MLVs) (\sim 0.3 mM phospholipid in phosphate-buffered saline) were prepared as previously described using microsomal lipid extracts from liver and brain tissue for at least three wild-type (WT) and three CerS2 null mice of different ages (6, 17). Fluorescence anisotropy was measured (at least 10 measurements for each analysis) in a FluoroLog[®]-3 fluorimeter (Horiba Jobin-Yvon, NJ) or an SLM Aminco 8100

series 2 spectrofluorimeter using t-PnA and Rho (at final probe concentrations of 0.7 μ M and 0.5 μ M, respectively). All measurements were performed at room temperature in 0.5 cm \times 0.5 cm quartz cuvettes under magnetic stirring. The excitation (λ_{ex})/emission (λ_{em}) wavelengths were 320/405 nm for t-PnA and 570/593 nm for Rho.

RESULTS

Sphingolipid composition of liver and brain microsomes

We previously demonstrated that CerS2 null mouse liver and brain exhibit a significantly altered SL composition but no major alterations in phospholipid and cholesterol composition (6, 8). We now characterize the SL profile of microsomal lipids obtained from liver and brain of control and CerS2 null mice of different ages. Microsomes were used as a source of lipids because they are free from contaminating lipid particles (such as LDL) in the case of liver or myelin in brain.

Microsomal brain lipids are enriched in Cer (Supplementary Fig. S1A) compared with whole brain where SM and hexosylceramide (HexCer), which consists of both glucosylceramide (GlcCer) and galactosylceramide (GalCer), predominate (8). Because HexCer, particularly GalCer (8), is the major SL in myelin, the enrichment of Cer and the low levels of HexCer in microsomal brain lipids demonstrate that the extracts have little or no myelin lipid contamination. This was further confirmed by Western blotting, in which myelin basic protein was barely detectable in the microsomal fractions, which were highly enriched in the ER marker, BiP (data not shown). Changes in the acyl chain composition of Cer, SM, and HexCer were similar in microsomes to whole brain (Supplementary Fig. S1A). Briefly, C18-SLs were elevated, and VLC-SLs were depleted (Fig. 1A and Supplementary Fig. S1). In addition, CerS2 null mice displayed a significant reduction in unsaturated SLs and an increase in saturated SLs (Fig. 1B). The reduction in unsaturated SLs is a consequence of CerS2 ablation because the major contribution to the total unsaturated SLs in the WT mouse is due to C24:1 species (\sim 14% of the total SLs), with a smaller fraction (\sim 3%) contributed by the C18:1 species. Long chain bases (LCBs) (mainly sphinganine) were also elevated in brain microsomes, but the mol% of LCBs was only 1.0 ± 0.2 of the total sphingolipids in microsomes from WT mice and 3.0 ± 1.0 mol% in microsomes from CerS null mice. Such low amounts are unlikely to affect the biophysical properties of the vesicles prepared from microsomal lipids.

The SL composition of microsomal liver lipids (Supplementary Fig. S2A) was similar to whole liver (6) (i.e., SM comprised \sim 50–60% of the total SLs), and HexCer was a minor component ($<$ 10%). A small increase in LCB levels was observed in CerS2 null liver microsomes ($4.0 \pm 1.3\%$) compared with $1.5 \pm 0.5\%$ in WT mice. As in whole liver, a significant shift in the acyl chain composition from VLC-SLs to LC-SLs (Fig. 1C) was observed in the CerS2 null mouse, with C16-SLs significantly elevated (Supplementary Figs. S2B, C). Similar to brain, a significant shift in the ratio of unsaturated to saturated SLs was observed, with the latter

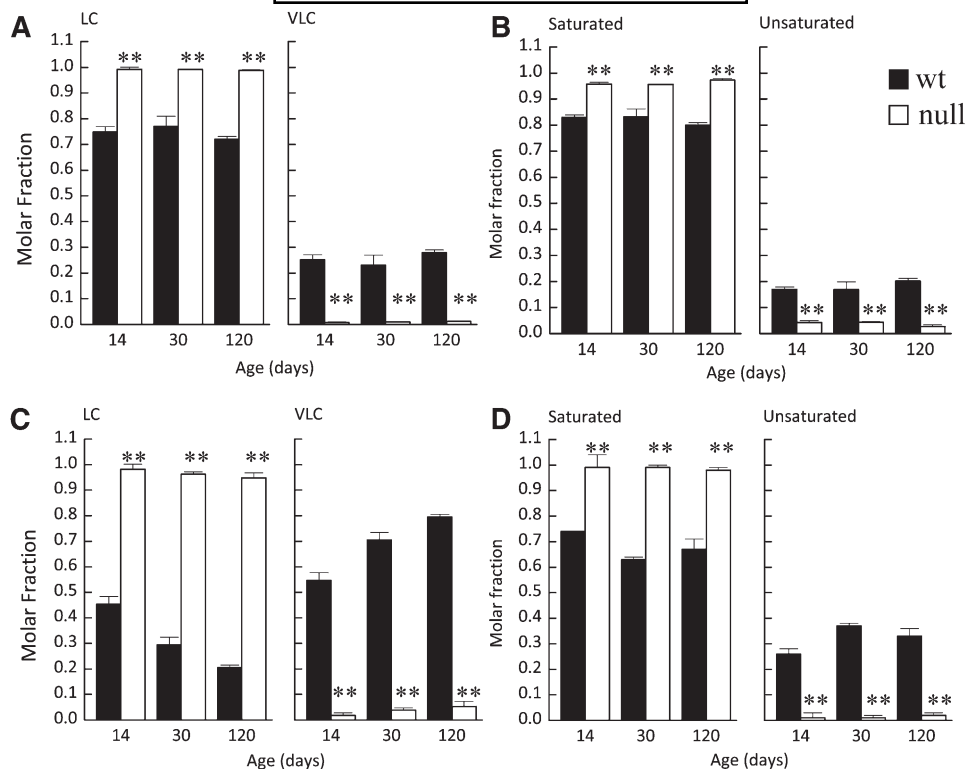


Fig. 1. LC-ESI MS/MS analysis of microsomal liver and brain lipids in WT and CerS2 null mice. Molar fractions of long (LC, A, C) and very long acyl chain (VLC) SLs and (B, D) saturated and unsaturated SLs from (A, B) brain or (C, D) liver of control (WT) and CerS2 null mice. Values are means \pm SD ($n \geq 3$). Each sample was measured in duplicate. ** $P < 0.01$.

much more prominent (Fig. 1D), due to the higher contribution of C24:1-SLs ($\sim 30\%$ of total SLs). Thus, ablation of CerS2 causes significant changes in the chain length of liver and brain microsomal SLs and also in their degree of saturation; the former should increase membrane fluidity (18), whereas the latter should promote an increase in membrane order (19). The balance between these changes should dictate the overall biophysical properties of the membranes.

Altered membrane morphology in CerS2 null mice

Giant unilamellar vesicles (GUVs) were prepared from liver and brain microsomal lipids and examined by microscopy. Control vesicles prepared from WT mice were present as stable isolated vesicles with a round shape typical of GUVs (Fig. 2A, B). In contrast, most vesicles prepared from CerS2 null mice showed morphological changes that included nonround-shaped vesicles containing areas of different curvature in the same vesicle and tubule-like structures emerging from a single vesicle (Fig. 2A, lower panel) or at contact points between two vesicles (Fig. 2B, lower panel). These vesicles were also highly dynamic, with a strong tendency to adhere and fuse with neighboring vesicles (Fig. 2A, B). As a consequence, the vesicles appeared as aggregates or as small vesicles inside bigger vesicles. Similar alterations were observed in brain (Fig. 2A) and liver (Fig. 2B), although vesicles derived from brain were less affected (see also Figs. 3 and 4). These results demonstrate that alterations in the SL acyl chain structure

and composition of CerS2 null mice compromise membrane lipid packing, promoting changes in membrane curvature and enhancing processes such as fusion and budding. Because there are no significant variations in phospholipid and cholesterol content between CerS2 null and control mice (6, 8), we conclude that the changes in biophysical properties are a direct consequence of changes in the SL composition.

Changes in membrane phases and phase separation in CerS2 null mouse brain

Alterations in the type of membrane phases and in the extent of phase separation were observed in lipids obtained from CerS2 null mouse brain. Vesicles were labeled with probes (i.e., NBD and Rho) that act as markers of liquid-ordered (lo) and liquid-disordered (ld) phases, respectively (17). Vesicles from WT mice (14 and 30 days old; Fig. 3A, B) were homogeneously labeled with both probes (except for small regions enriched in Rho), resulting in a yellow-colored overlay containing small red-colored areas enriched in Rho, which correspond to less-packed lipid domains. The area occupied by these domains changes with the age of the mice, resulting in alterations in global membrane order, as observed by the variation in t-PnA and Rho fluorescence anisotropy (Fig. 3D, E). In contrast, vesicles from CerS2 null mice displayed lo-ld phase separation, resulting in an overlay image with large and distinct green (lo) and red (ld) areas. The extent of ld-lo phase separation also changes with mouse age. The increase in

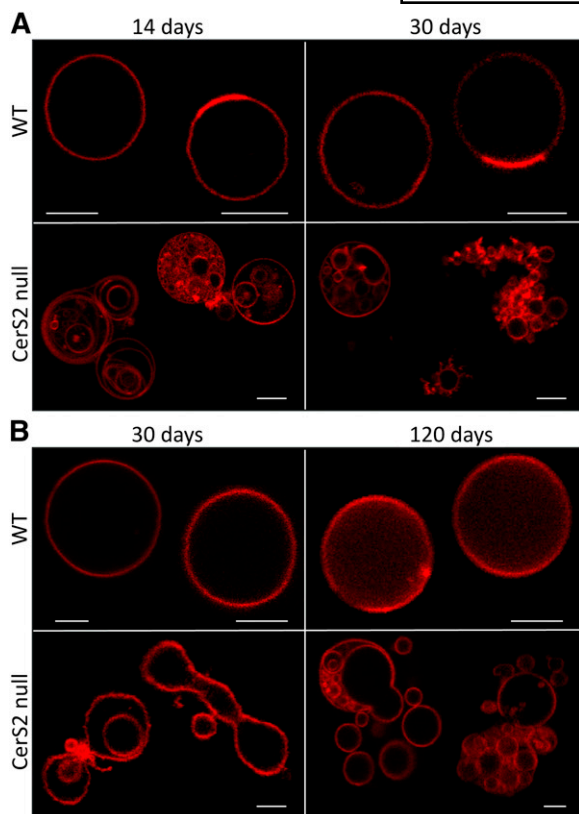


Fig. 2. Effect of CerS2 ablation on membrane morphology. Confocal fluorescence microscopy of GUVs prepared from microsomal lipids from (A) brain or (B) liver of control (upper panels) and CerS2 null (lower panels) mice of different ages. GUVs were labeled with Rho. Scale bar, 5 μ m.

the lo phase, and therefore in the global order of the membrane, was further detected by the increase in fluorescence anisotropy of t-PnA at 30 days of age (Fig. 3D, E). In older CerS2 null mice, the extent of ld-lo phase separation is lower (Fig. 3C), but t-PnA anisotropy shows an increase in membrane order (Fig. 3F) due to formation of small gel-like domains that appear as dark areas (areas which exclude NBD and Rho) (Fig. 3C). The partitioning of t-PnA into these gel-like domains (20) results in a significant increase in anisotropy, which reflects gel domain formation rather than a global increase in membrane order of a fluid phase membrane. A similar increase in membrane order is observed in 120 day-old WT mice, which is also due to formation of small scattered gel-like domains. Despite the similar increase in membrane order in WT and older CerS2 null mice, fluorescence microscopy images show distinctive morphological features.

To further monitor changes in membrane order, the fluorescence anisotropy of Rho was measured. Rho anisotropy is affected by energy homotransfer, causing a decrease in anisotropy, with the process depending on the surface concentration of the probes. This is associated with an increase in membrane order [e.g., formation of lo or gel domains (17)], leading to probe exclusion from the more ordered regions (Fig. 3A, B), thereby inducing closer localization in the more fluid regions as occurs in vesicles from CerS2 null brain in younger mice (Fig. 3D, E). In older

mice (Fig. 3C), the more homogeneous distribution of Rho results in a slight increase in Rho anisotropy (Fig. 3F), which is due to the increased area available for probe distribution. Simultaneously, a decrease in the lo phase results in a decrease in global membrane order. Thus, CerS2 ablation promotes alterations in the type and extent of phase separation of brain lipids, which leads to changes in the local and global order of the membrane.

Increased membrane fluidity in CerS2 null mouse liver

Fluorescence microscopy of vesicles obtained from WT and CerS2 null liver membranes (Fig. 4A, B) demonstrated a relatively homogeneous distribution of NBD and Rho, with small NBD-enriched, Rho-free areas corresponding to more ordered domains. The lo domains were present in WT and CerS2 null membranes irrespective of mouse age. Noteworthy differences were observed in membrane order (Fig. 4C, D), with the lower t-PnA anisotropy in CerS2 null mouse consistent with increased membrane fluidity, as previously demonstrated (6) and consistent with the higher anisotropy of Rho. These results suggest an overall decrease in membrane order in lipids from CerS2 null mice. The increased fluidity might be associated with the morphological alterations, consistent with observations showing that the lower bending rigidity of the ld phase facilitates formation of highly curved structures (21) such as tubules.

DISCUSSION

In the present study we have shown that ablation of CerS2 leads to changes in SL levels that cause alterations in various membrane biophysical properties, such as fluidity, type of phases, the extent of phase separation, and membrane curvature and morphology. The changes were tissue dependent, which is related to the different changes in SL acyl chain and composition between liver and brain.

In membranes derived from microsomal lipids from liver, fluidity was increased in the CerS2 null mouse. This change in fluidity is due to a combination of several factors, including the reduction in VLC-SL and the increase in C16-SL. LC-SLs have a lower melting temperature (18, 22), which might contribute to the higher fluidity. In contrast, lipids with a higher melting temperature have a strong tendency to segregate into gel domains, which would contribute to the increase in the global order of the membrane (23, 24). In contrast, the increase in saturated SLs, which induce a considerable degree of order, may counteract the effect of decreasing VLC-SLs in such a way that the changes in membrane fluidity are not as large as would be expected if only one of the parameters had changed. The increase in LCB levels could also cause an increase in membrane order and in stabilization of raft domains, but higher levels are required to cause such effects (25, 26). Irrespective of the extent or the cause of the change in membrane fluidity, changes in membrane morphology are induced. Low membrane bending rigidity, such as occurs in disordered phases (21), enhances formation of curved structures. Liver membranes from

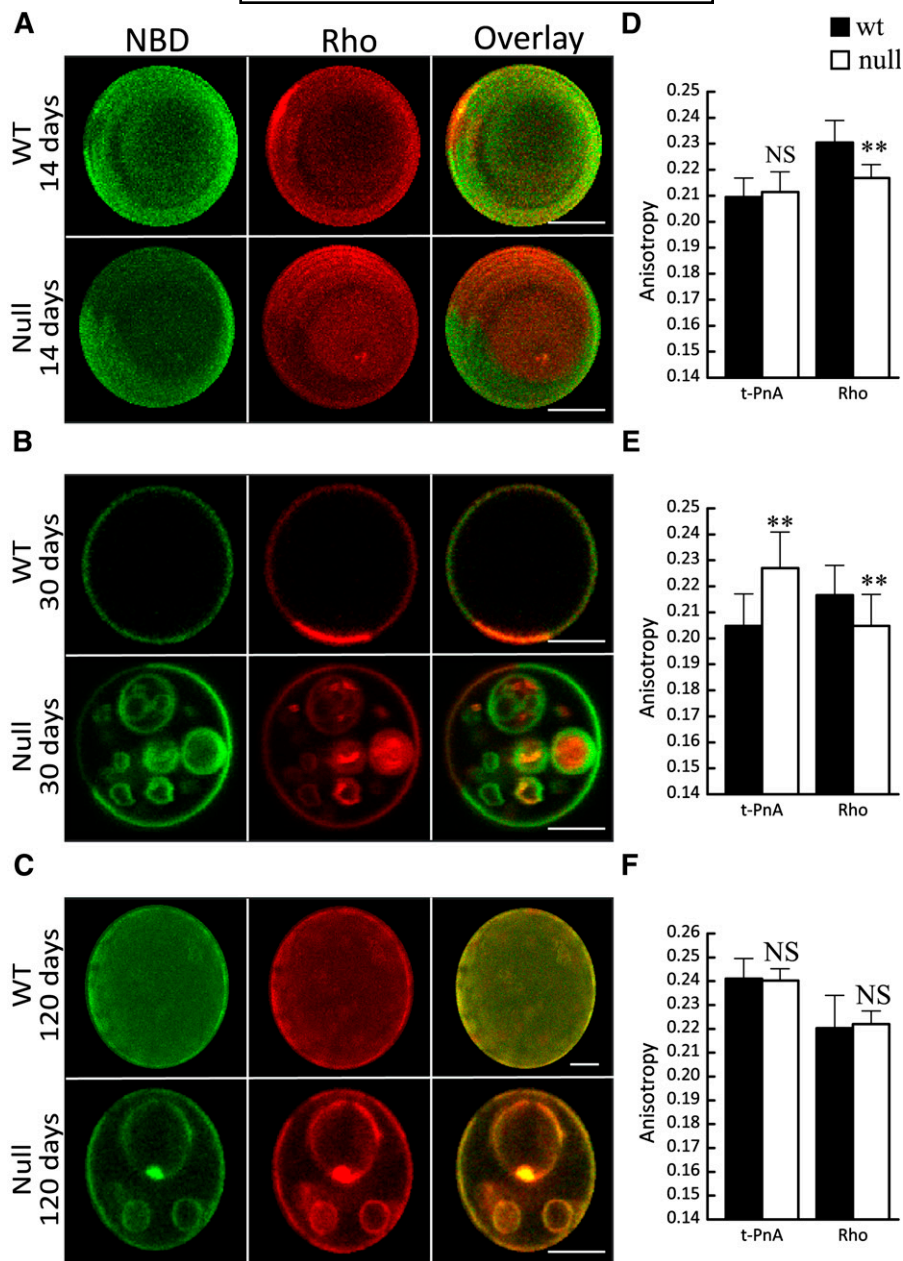


Fig. 3. Effect of CerS2 ablation on biophysical properties of brain membranes. A–C: Confocal fluorescence microscopy of control (upper panels, WT) and CerS2 null (lower panels, CerS2 null) mice from (A) 14, (B) 30, and (C) 120 day-old mice. NBD (green) and Rho (red) were used to label lo and ld phases, respectively. The overlay image shows (i) areas of colocalization (yellow), (ii) areas of segregation (dark regions), (iii) NBD alone (green), and (iv) Rho alone (red). A and C (upper row): 3D projections obtained from confocal slices of the GUVs. Scale bar, 5 μ m. D–F: Fluorescence anisotropy of t-PnA and Rho in WT and CerS2 null mice that were (D) 14, (E) 30, and (F) 120 days old. Values are the means \pm SD ($n \geq 3$). Fluorescence anisotropy was measured at least 10 times for each sample. $**P < 0.01$.

CerS2 null mice had a higher tendency to adhere and fuse with neighboring vesicles and/or to bud from bigger vesicles, processes that require changes in membrane curvature, which could be achieved by lipid phase separation where sorting of lipids that promote the formation of curved structures takes place (27).

One of the most interesting observations in brain membranes was the complete segregation of ld and lo phases in vesicles from CerS2 null mice. Moreover, the extent of the lo phase was increased compared with WT mice, resulting

in increased membrane order, which can be attributed to depletion of unsaturated SLs. The decrease in VLC-SLs in brain membranes was not as large as in liver because brain is enriched in LC-SLs (8), such that the length of the acyl chains contributes less to the increased membrane fluidity. Despite the lower fluidity of CerS2 null brain membranes, altered morphology was also observed. Changes in membrane morphology in liver and brain are probably related to similar changes that occur in each type of tissue, such as depletion of VLC- and unsaturated SLs.

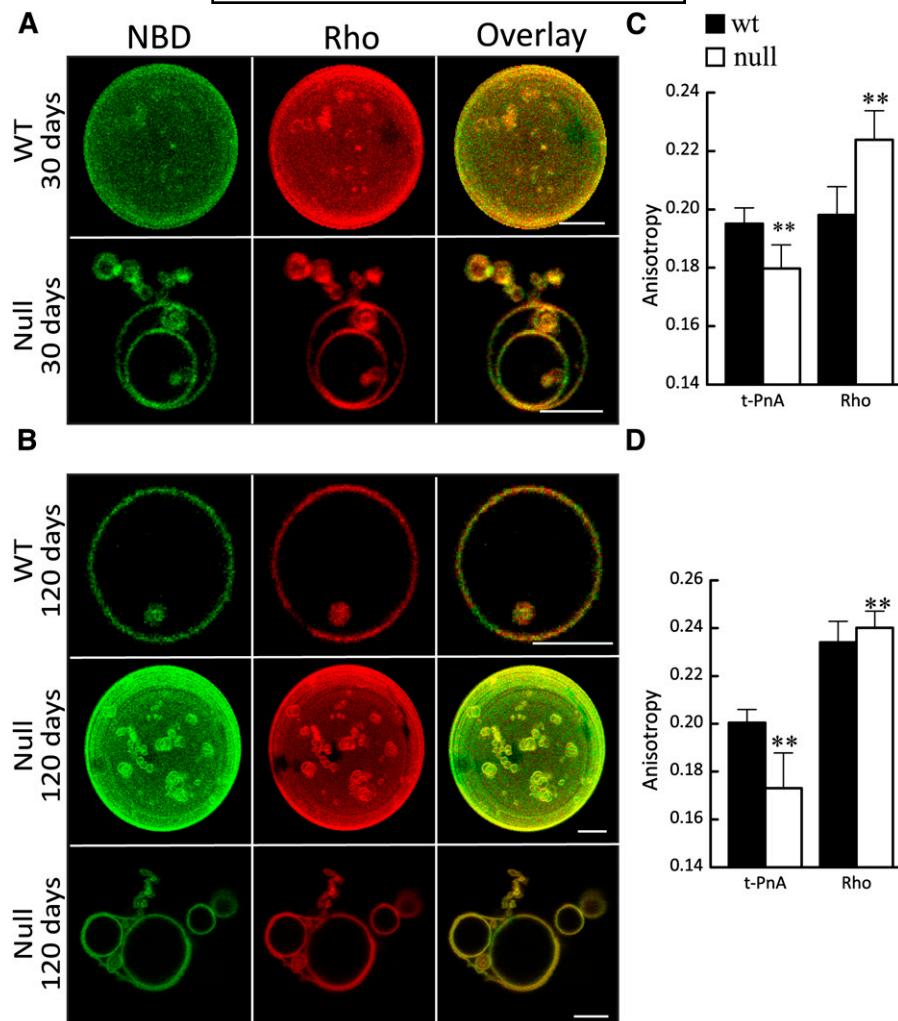


Fig. 4. Effect of CerS2 ablation on biophysical properties of liver membranes. A, B: Confocal fluorescence microscopy of control (upper panels) and CerS2 null (middle and lower panels) mice that were (A) 30 and (B) 120 days of age. NBD (green) and Rho (red) were used to label lo and ld phases, respectively. A (upper row) and B (middle row): 3D projections obtained from confocal slices of the GUVs. Scale bar, 5 μ M. C, D: Fluorescence anisotropy of t-PnA and Rho in WT and CerS2 null mice that were (D) 30 and (E) 120 days old. Values are means \pm SD ($n \geq 3$). Fluorescence anisotropy was measured at least 10 times for each sample. ** $P < 0.01$.

This is one of the first studies to examine differences in membrane biophysical properties in natural membranes enriched in SLs with specific acyl chain structures. Such changes as reported herein may influence a variety of cellular functions, including activation/inhibition of specific signaling proteins that undergo conformational changes upon membrane physical alterations (28, 29). Moreover, the existence of membrane domains with phase properties distinct from the bulk membrane is often associated with entrapment therein of ligands and receptors in order to amplify signal transduction (30) or to the activation of certain enzymes by facilitating their adsorption on the membrane at the interfacial defects between the two phases (31). In cell membranes, formation of such domains may occur transiently due to the constant lipid and protein re-shuffling by cellular processes such as synthesis/degradation, flip-flop, and trafficking (32, 33).

Of no less importance are the changes that occur in membrane morphology. Changes in membrane morphology are

closely dependent on membrane mechanics such as tension, shear stress, hydrostatic pressure, and compression (34). Cellular processes that depend on membrane mechanics and morphology, such as endocytosis-exocytosis (35, 36), fusion, and budding (32, 37), may be impaired in the CerS2 null mouse. Impairment of these processes has significant implications on the sorting of lipids and proteins and in the development and maintenance of organelles such as the ER and Golgi (38–40). Thus, alterations in the curvature and fluidity of the membrane might have important ramifications on cell physiology (13, 41). For instance, deficient trafficking might drive accumulation of lipids in the lysosomes, ultimately leading to lysosomal storage diseases (10, 42). Banana-shaped storage material, similarly to that observed in neurons of GM1 gangliosidosis mouse (43), was detected in lysosomes of astrocytes from the brain of CerS2 null mouse (8).

In summary, ablation of CerS2 affects SL metabolism to different extents in liver and brain, causing significant

alterations in the global order of the membrane, in the extent of phase separation, and in the number and type of lipid domains formed and causes major changes in membrane morphology. The study of membrane biophysical properties paves the way for understanding the impact of SL acyl chain structure on various membrane properties in general and more specifically for defining the cellular mechanisms of pathology in CerS2 null mice. **■**

REFERENCES

1. Futerman, A. H., and H. Riezman. 2005. The ins and outs of sphingolipid synthesis. *Trends Cell Biol.* **15**: 312–318.
2. Futerman, A. H., and Y. A. Hannun. 2004. The complex life of simple sphingolipids. *EMBO Rep.* **5**: 777–782.
3. Pewzner-Jung, Y., S. Ben Dor, and A. H. Futerman. 2006. When do lasses (longevity assurance genes) become CerS (Ceramide Synthases)? Insights into the regulation of ceramide synthesis. *J. Biol. Chem.* **281**: 25001–25005.
4. Laviad, E. L., L. Albee, I. Pankova-Kholmyansky, S. Epstein, H. Park, A. H. Merrill, and A. H. Futerman. 2008. Characterization of ceramide synthase 2. *J. Biol. Chem.* **283**: 5677–5684.
5. Levy, M., and A. H. Futerman. 2010. Mammalian ceramide synthases. *IUBMB Life.* **62**: 347–356.
6. Pewzner-Jung, Y., H. Park, E. L. Laviad, L. C. Silva, S. Lahiri, J. Stiban, R. Erez-Roman, B. Brugger, T. Sachsenheimer, F. Wieland, et al. 2010. A critical role for ceramide synthase 2 in liver homeostasis: I. Alterations in lipid metabolic pathways. *J. Biol. Chem.* **285**: 10902–10910.
7. Pewzner-Jung, Y., O. Brenner, S. Braun, E. L. Laviad, S. Ben Dor, E. Feldmesser, S. Horn-Saban, D. Amann-Zalcenstein, C. Raanan, T. Berkutzi, et al. 2010. A critical role for ceramide synthase 2 in liver homeostasis: II. Insights into molecular changes leading to hepatopathy. *J. Biol. Chem.* **285**: 10911–10923.
8. Ben-David, O., Y. Pewzner-Jung, O. Brenner, E. L. Laviad, A. Kogot-Levin, I. Weissberg, I. E. Biton, R. Pienik, E. Wang, S. Kelly, et al. 2011. Encephalopathy caused by ablation of very long acyl chain ceramide synthesis may be largely due to reduced galactosylceramide levels. *J. Biol. Chem.* **286**: 30022–30033.
9. van Meer, G., and H. Sprong. 2004. Membrane lipids and vesicular traffic. *Curr. Opin. Cell Biol.* **16**: 373–378.
10. Ballabio, A., and V. Gieselmann. 2009. Lysosomal disorders: from storage to cellular damage. *Biochim. Biophys. Acta.* **1793**: 684–696.
11. Grassmé, H., J. Riethmüller, and E. Gulbins. 2007. Biological aspects of ceramide-enriched membrane domains. *Prog. Lipid Res.* **46**: 161–170.
12. Simons, K., and D. Toomre. 2000. Lipid rafts and signal transduction. *Nat. Rev. Mol. Cell Biol.* **1**: 31–39.
13. Heinrich, M., A. Tian, C. Esposito, and T. Baumgart. 2010. Dynamic sorting of lipids and proteins in membrane tubes with a moving phase boundary. *Proc. Natl. Acad. Sci. USA.* **107**: 7208–7213.
14. Folch, J., M. Lees, and G. H. Stanley. 1957. A simple method for the isolation and purification of total lipids from animal tissues. *J. Biol. Chem.* **226**: 497–509.
15. Shaner, R. L., J. C. Allegood, H. Park, E. Wang, S. Kelly, C. A. Haynes, M. C. Sullards, and A. H. Merrill. 2009. Quantitative analysis of sphingolipids for lipidomics using triple quadrupole and quadrupole linear ion trap mass spectrometers. *J. Lipid Res.* **50**: 1692–1707.
16. Pinto, S. N., L. C. Silva, R. F. M. de Almeida, and M. J. Prieto. 2008. Membrane domain formation, interdigitation and morphological alterations induced by the very long chain asymmetric C24:1 ceramide. *Biophys. J.* **95**: 2867–2879.
17. Silva, L. C., A. H. Futerman, and M. Prieto. 2009. Lipid raft composition modulates sphingomyelinase activity and ceramide-induced membrane physical alterations. *Biophys. J.* **96**: 3210–3222.
18. Niemelä, P. S., M. T. Hyvonen, and I. Vattulainen. 2006. Influence of chain length and unsaturation on sphingomyelin bilayers. *Biophys. J.* **90**: 851–863.
19. Björkqvist, Y. J., J. Brewer, L. A. Bagatoli, J. P. Slotte, and B. Westerlund. 2009. Thermotropic behavior and lateral distribution of very long chain sphingolipids. *Biochim. Biophys. Acta.* **1788**: 1310–1320.
20. Sklar, L. A., G. P. Miljanich, and E. A. Dratz. 1979. phospholipid lateral phase-separation and the partition of Cis-parinaric acid and trans-parinaric acid among aqueous, solid lipid, and fluid lipid phases. *Biochemistry.* **18**: 1707–1716.
21. Roux, A., D. Cuvelier, P. Nassoy, J. Prost, P. Bassereau, and B. Goud. 2005. Role of curvature and phase transition in lipid sorting and fission of membrane tubules. *EMBO J.* **24**: 1–9.
22. Marsh, D. 1990. Handbook of lipid bilayers. CRC Press, Boca Raton, FL.
23. Pinto, S. N., L. C. Silva, A. H. Futerman, and M. Prieto. 2011. Effect of ceramide structure on membrane biophysical properties: the role of acyl chain length and unsaturation. *Biochim. Biophys. Acta.* **1808**: 2753–2760.
24. Silva, L., R. F. M. De Almeida, A. Fedorov, A. P. A. Matos, and M. Prieto. 2006. Ceramide-platform formation and -induced biophysical changes in a fluid phospholipid membrane. *Mol. Membr. Biol.* **23**: 137–148.
25. Lopez-Garcia, F., J. Villalain, and J. C. Gomez-Fernández. 1994. A phase behavior study of mixtures of sphingosine with zwitterionic phospholipids. *Biochim. Biophys. Acta.* **1194**: 281–288.
26. Georgieva, R., K. Koumanov, A. Momchilova, C. Tessier, and G. Staneva. 2010. Effect of sphingosine on domain morphology in giant vesicles. *J. Colloid Interface Sci.* **350**: 502–510.
27. Goñi, F. M., and A. Alonso. 2009. Effects of ceramide and other simple sphingolipids on membrane lateral structure. *Biochim. Biophys. Acta.* **1788**: 169–177.
28. Reynwar, B. J., G. Illya, V. A. Harmandaris, M. M. Muller, K. Kremer, and M. Deserno. 2007. Aggregation and vesiculation of membrane proteins by curvature-mediated interactions. *Nature.* **447**: 461–464.
29. Hatzakis, N. S., V. K. Bhatia, J. Larsen, K. L. Madsen, P. Y. Bolinger, A. H. Kunding, J. Castillo, U. Gether, P. Hedegard, and D. Stamou. 2009. How curved membranes recruit amphipathic helices and protein anchoring motifs. *Nat. Chem. Biol.* **5**: 835–841.
30. Rajendran, L., and K. Simons. 2005. Lipid rafts and membrane dynamics. *J. Cell Sci.* **118**: 1099–1102.
31. Maggio, B., G. A. Borioli, M. Del Boca, L. De Tullio, M. L. Fanani, R. G. Oliveira, C. M. Rosetti, and N. Wilke. 2008. Composition-driven surface domain structuring mediated by sphingolipids and membrane-active proteins. *Cell Biochem. Biophys.* **50**: 79–109.
32. van Meer, G., D. R. Voelker, and G. W. Feigenson. 2008. Membrane lipids: where they are and how they behave. *Nat. Rev. Mol. Cell Biol.* **9**: 112–124.
33. Kusumi, A., and K. Suzuki. 2005. Toward understanding the dynamics of membrane-raft-based molecular interactions. *Biochim. Biophys. Acta.* **1746**: 234–251.
34. Janmey, P. A., and C. A. McCulloch. 2007. Cell mechanics: integrating cell responses to mechanical stimuli. *Annu. Rev. Biomed. Eng.* **9**: 1–34.
35. Keren, K. 2011. Membrane tension leads the way. *Proc. Natl. Acad. Sci. USA.* **108**: 14379–14380.
36. Apodaca, G. 2002. Modulation of membrane traffic by mechanical stimuli. *Am. J. Physiol. Renal Physiol.* **282**: F179–F190.
37. Rustom, A., R. Saffrich, I. Markovic, P. Walther, and H. H. Gerdes. 2004. Nanotubular highways for intercellular organelle transport. *Science.* **303**: 1007–1010.
38. Spang, A. 2009. On vesicle formation and tethering in the ER–Golgi shuttle. *Curr. Opin. Cell Biol.* **21**: 531–536.
39. Boot, R. G., M. Verhoeck, W. Donker-Koopman, A. Strijland, J. van Marle, H. S. Overkleeft, T. Wennekes, and J. M. F. G. Aerts. 2007. Identification of the non-lysosomal glucosylceramidase as beta-glucosidase 2. *J. Biol. Chem.* **282**: 1305–1312.
40. Aridor, M. 2007. Visiting the ER: the endoplasmic reticulum as a target for therapeutics in traffic related diseases. *Adv. Drug Deliv. Rev.* **59**: 759–781.
41. Donaldson, J. G. 2009. Phospholipase D in endocytosis and endosomal recycling pathways. *Biochim. Biophys. Acta.* **1791**: 845–849.
42. Kirkegaard, T., and M. Jaattella. 2009. Lysosomal involvement in cell death and cancer. *Biochim. Biophys. Acta.* **1793**: 746–754.
43. Boomkamp, S. D., and T. D. Butters. 2008. Glycosphingolipid disorders of the brain. *In* Lipids in health and disease. P. J. Quinn and X. Wang, editors. Springer, The Netherlands. 441–467.